Stream Temperature Dynamics in Upland Agricultural Watersheds

By M. Younus,[1] M. Hondzo,[2] and B. A. Engel[3]

ABSTRACT: A numerical model to compute the free-surface flow hydrodynamics and stream temperature dynamics by solving the depth-averaged, 1D unsteady flow and heat transport equations is presented. The hydrodynamics model considers the effects of arbitrary stream geometry, variable slopes, variable flow regimes, and unsteady boundary conditions. The thermal transport model accounts for the effects of solar radiation, air temperature, relative humidity, cloud cover, wind speed, heat conduction between water and streambed, subsurface flow, and shading by riparian vegetation. The model is verified with measurements in a stream in an upland agricultural watershed located in Indiana. Diurnal variations in the streamflow and stream temperatures are highly transient. The proposed model predicted well the streamflow and stream temperatures that were measured every 15 min over 25 days. The results of this study demonstrate that the solar (shortwave) radiation and subsurface inflow are the most significant contributors to the stream heat budget.

INTRODUCTION

The rate of chemical reactions as well as the biological activity is mediated by water temperature in aquatic systems. Higher water temperature usually implies faster chemical reactions and more active biological activity in aquatic environments (Chapra 1997). Fish survival and growth potential are significantly influenced by water temperature. For all of the above reasons, water temperature is considered to be a physical frame for aquatic environments.

The accuracy and potential success of any ecological or water quality model hinges upon the proper description of the heat exchange between the water and surrounding environment. Therefore, considerable effort has been devoted to field measurements (Contantz 1998; Ronan et al. 1998) as well as to formulation of numerical models (Sinokrot and Stefan 1993; Kim and Chapra 1997; Polehn and Kinsel 1997; Chen et al. 1998a,b) for water temperature prediction in aquatic environments. Prediction models range from regression similar to air-water predictors (Stefan and Preud'homme 1993; Webb and Nobilis 1997; Mohseni et al. 1998) to heat advection/dispersion descriptions (Sinokrot and Stefan 1993; Kim and Chapra 1997). The regression models, although very simple, have been successful at weekly timescales. However, stream water temperature fluctuates at hourly and daily timescales. The heat advection/dispersion transport models with full consideration of inflow and outflow boundary conditions are unavoidable for the daily or hourly timescales (Sinokrot and Stefan 1993). In upland agricultural watersheds, flow rate in small streams is abrupt and unsteady for a given storm event (Kim 1996). An example of the measured streamflow in Little Pine Creek, located in an upland agricultural watershed in north-central Indiana, is given in Fig. 1. Clearly, unsteady flow is a characteristic feature rather than a case in the stream. Flat peaks in the hydrograph are indicators of overbank flow. Kim and Chapra (1997) coupled a 1D heat transport model with a simplified hydrodynamic model for unsteady flow. The inertia terms were neglected in the momentum equation, and the

[1]Water Resour. Engr., Christopher B. Burke Engineering, Ltd., 9575 West Higgins Rd., Ste. 600, Rosemont, IL 60018.

[2]Assoc. Prof., St. Anthony Falls Lab., Dept. of Civ. Engrg., Univ. of Minnesota, Minneapolis, MN 55414-2196.

[3]Prof., Dept. of Agric. and Biol. Engrg., Purdue Univ., West Lafayette, IN 47907.

model was successfully applied in a steep channel where temporal change in flow is not abrupt. The solution of the complete hydrodynamics equation is necessary to incorporate the inertial terms, variety of channel slopes, and abrupt boundary conditions in small streams.

In this paper, fully hydrodynamic and heat transport models are developed and coupled for water temperature and streamflow prediction in streams. The model considers air-water heat exchange, sediment-water heat exchange, lateral heat inflow/outflow, subsurface inflow/outflow, and the interaction between solar radiation and riparian vegetation. The proposed model is verified with measurements in Little Pine Creek, Tippecanoe County, Ind. Good agreement between field measurements and model prediction is reported.

METHODOLOGY

Hydrodynamics

Governing Equations

The 1D equations based on the conservation of mass and momentum can be used to describe the unsteady free-surface flow caused by a storm in an upland agricultural watershed. For a channel having a general cross section with small slope, the equations in the conservation form (Chaudhry 1993) may be written as follows:

$$\frac{\partial A}{\partial t} + \frac{\partial Q}{\partial x} = q_x \qquad (1)$$

$$\frac{\partial Q}{\partial t} + \frac{\partial}{\partial x}(QV + gA\bar{y}) = gA(S_o - S_f) \qquad (2)$$

where A = area of cross section (m^2); Q = flow rate (m^3/s); q_x = lateral inflow per unit stream length (m^2/s); t = time (s); x = distance along the channel (m); g = acceleration due to gravity (m/s^2); V = velocity of flow (m/s); $\bar{y}$ = depth to the centroid of the channel section (m); S_o = slope of the channel bed (m/m); and S_f = friction slope (m/m).

Numerical Solution

The governing equations [(1) and (2)] are a system of mixed nonlinear hyperbolic and parabolic partial differential equations (Abbot 1979). These equations may be solved by using the method of characteristics, finite-difference, finite-element, finite-volume, and spectral approaches. The finite-difference methods have been the primary solution procedure for (1) and (2) (Fennema and Chaudhry 1989).

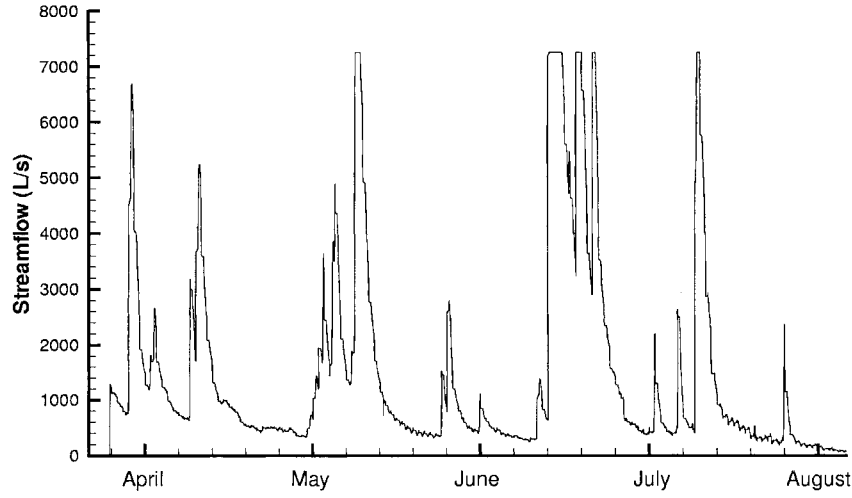The implicit switching scheme developed by Beam and

FIG. 1. Streamflow (L/s) over 232 Days at Downstream (825W) Gauging Station on Little Pine Creek, Ind., 1998

Warming (1976, 1978) is used in this study. Fennema and Chaudhry (1987) used the scheme to compute 1D dam-break flow for a rectangular cross section. Younus and Chaudhry (1994) used a similar scheme for 2D free-surface flow. A description of the method for a channel having a general cross section, unsteady, and 1D flow is given below.

The governing equations [(1) and (2)] may be written in the vector form as

$$\frac{\partial \mathbf{U}}{\partial t} + \frac{\partial \mathbf{F}}{\partial x} + \mathbf{S} = 0 \tag{3}$$

where

$$\mathbf{U} = \begin{bmatrix} A \\ Q \end{bmatrix}, \quad \mathbf{F} = \begin{bmatrix} Q \\ QV + gA\bar{y} \end{bmatrix}, \quad \mathbf{S} = \begin{bmatrix} -q_x \\ -gA(S_o - S_f) \end{bmatrix}$$

Eq. (3) may be solved by using the time difference approximation of the general form

$$\frac{\partial \mathbf{U}}{\partial t} \simeq \frac{\mathbf{U}^{n+1} - \mathbf{U}^n}{\Delta t} = \left(\frac{\Delta \mathbf{U}}{\Delta t}\right)^{n+1}$$

$$= \frac{\theta_1}{1 + \theta_2}\left(\frac{\partial \mathbf{U}}{\partial t}\right)^{n+1} + \frac{1 - \theta_1}{1 + \theta_2}\left(\frac{\partial \mathbf{U}}{\partial t}\right)^{n} + \frac{\theta_2}{1 + \theta_2}\left(\frac{\partial \mathbf{U}}{\partial t}\right)^{n-1} \tag{4}$$

where θ_1 and θ_2 = temporal weighting parameters leading to a variety of solution schemes (Younus and Chaudhry 1994). Solution for $\partial \mathbf{U}/\partial t$ from (3) and substitution in (4) yields

$$\Delta \mathbf{U}^{n+1} + \frac{\theta_1 \Delta t}{1 + \theta_2}\left[\frac{\partial(\Delta \mathbf{F}^{n+1})}{\partial x} + \Delta \mathbf{S}^{n+1}\right]$$

$$= -\frac{\Delta t}{1 + \theta_2}\left[\frac{\partial \mathbf{F}^n}{\partial x} + \mathbf{S}^n\right] + \frac{\theta_2}{1 + \theta_2}\Delta \mathbf{U}^{n-1} \tag{5}$$

Eq. (5) is nonlinear, because $\Delta \mathbf{F}^{n+1}$ and $\Delta \mathbf{S}^{n+1}$ are unknown nonlinear functions of the dependent variables. This equation must, therefore, be linearized before solving by an implicit finite-difference method. This is done by expanding each nonlinear term in the Taylor series about the unknown time (Younus and Chaudhry 1994). By expanding $\mathbf{F}^{n+1}$ and $\mathbf{S}^{n+1}$ in Taylor series and substituting in (5), we get

$$\Delta \mathbf{U}^{n+1} + \frac{\theta_1 \Delta t}{1 + \theta_2}\left[\frac{\partial}{\partial x}(\mathbf{A}^n \Delta \mathbf{U}^{n+1}) + \mathbf{B}^n \Delta \mathbf{U}^{n+1}\right]$$

$$= -\frac{\Delta t}{1 + \theta_2}\left[\frac{\partial \mathbf{F}^n}{\partial x} + \mathbf{S}^n\right] + \frac{\theta_2}{1 + \theta_2}\Delta \mathbf{U}^{n-1} \tag{6}$$

where $\mathbf{A} = \partial \mathbf{F}/\partial \mathbf{U}$ and $\mathbf{B} = \partial \mathbf{S}/\partial \mathbf{U}$.

By using the method of characteristics, it can be shown that in free-surface flow, the information is transmitted only from the upwind direction in supercritical flow and from opposite directions in subcritical flow (Fennema and Chaudhry 1987). This effect, in a finite-difference scheme, is achieved by using the split flux algorithm as follows. The eigenvalues of the Jacobian matrix $\mathbf{A}$ are $\lambda_i = V \pm \sqrt{gd}$, where $i = 1, 2$; and $d =$ hydraulic depth (m). Suppose $\mathbf{D}$ is a diagonal matrix with eigenvalues of $\mathbf{A}$, and $\mathbf{M}$ is the matrix that has its columns with the eigenvector of $\mathbf{A}$. Then $\mathbf{A}$ has similarity transform (Warming and Beam 1978)

$$\mathbf{A} = \mathbf{M}\mathbf{D}\mathbf{M}^{-1} = \mathbf{M}\mathbf{D}^+\mathbf{M}^{-1} + \mathbf{M}\mathbf{D}^-\mathbf{M}^{-1} = \mathbf{A}^+ + \mathbf{A}^- \tag{7}$$

where $\mathbf{D}^+$ = diagonal matlrix with values max(λ_i, 0); and $\mathbf{D}^-$ = diagonal matrix with values min(λ_i, 0). Substituting (7) into (6) and rearranging, we get

$$\Delta \mathbf{U}^{n+1} + \frac{\theta_1 \Delta t}{1 + \theta_2}\left[\frac{\partial}{\partial x}(\mathbf{A}^{+n}\Delta \mathbf{U}^{n+1}) + \frac{\partial}{\partial x}(\mathbf{A}^{-n}\Delta \mathbf{U}^{n+1})\right]$$

$$+ \frac{\theta_1 \Delta t}{1 + \theta_2}(\mathbf{B}^n \Delta \mathbf{U}^{n+1}) = -\frac{\Delta t}{1 + \theta_2}\left[\left(\mathbf{A}^+\frac{\partial \mathbf{U}}{\partial x} + \mathbf{A}^-\frac{\partial \mathbf{U}}{\partial x}\right)^n + \mathbf{S}^n\right]$$

$$+ \frac{\theta_2}{1 + \theta_2}\Delta \mathbf{U}^{n-1} \tag{8}$$

By using the backward difference for $\mathbf{A}^+$ and the forward difference for $\mathbf{A}^-$ in (8) and simplifying, we get

$$\mathbf{a}_i \Delta \mathbf{U}_{i-1} + \mathbf{b}_i \Delta \mathbf{U}_i + \mathbf{c}_i \Delta \mathbf{U}_{i+1} = \mathbf{d}_i \tag{9}$$

Eq. (9) forms a block tridiagonal matrix system and is solved by using a modified Thomas algorithm (Younus and Chaudhry 1994).

Heat Transport

Governing Equation

Applying the principle of conservation of thermal energy to 1D well-mixed shallow open channel flow, the heat transport equation may be represented in nonconservation form as follows (Holley and Jirka 1986):

$$\frac{\partial T}{\partial t} + V\frac{\partial T}{\partial x} = \frac{1}{A}\frac{\partial}{\partial x}\left(AD\frac{\partial T}{\partial x}\right) + \frac{q_x}{A}(T_\ell - T) + \frac{H_t w}{C_w \rho_w A} + \frac{H_{sed} p}{C_w \rho_w A} \tag{10}$$

where T = average water temperature (°C); T_ℓ = lateral water temperature (°C); H_t = surface heat flux (W/m²); H_{sed} = heat

flux to/from sediment (W/m^2); D = longitudinal dispersion coefficient (m^2/s); C_w = specific heat of water (J/kg °C); ρ_w = density of water (kg/m^3); w = width of channel (m); and p = wetted perimeter of the channel (m).

Heat Balance Components

In (10), H_t accounts for the thermal energy flux transfer with the surrounding environment, and can be represented by

$$H_t = H_s + H_a - H_w - H_e - H_c \qquad (11)$$

$$H_s = (1 - R_t)(1 - S_h)H_{si} \qquad (12)$$

$$S_h = S_t + S_v \qquad (13)$$

where H_s = solar radiation entering water (W/m^2); R_t = solar radiation reflectivity coefficient (decimal); H_{si} = measured solar radiation (W/m^2); S_h = total riparian shading factor; S_t = topographic shade; S_v = vegetation shade; H_a = longwave radiation emitted by air (W/m^2); H_w = longwave radiation emitted by water (W/m^2); H_e = evaporation heat flux (W/m^2); and H_c = conductive heat flux (W/m^2). The expressions for H_a, H_w, H_e, and the algorithm used to compute shading factor are given by Theurer et al. (1984). The conduction heat flux was computed by using an expression given by Rasmussen et al. (1995).

Streambed Heat Flux

The heat conduction equation for a streambed can be specified as follows:

$$\rho_s c_p \frac{\partial T_b}{\partial t} = k_b \frac{\partial^2 T_b}{\partial z^2} \qquad (14)$$

where T_b = riverbed temperature (°C); ρ_s = density of streambed sediment (kg/m^2); c_p = specific heat of streambed sediment (J/kg°C); k_b = heat conductivity of the streambed (W/°C·m); and z = vertical distance from the streambed (m). The solution of (14) represents a profile of streambed temperature along the vertical distance. This distribution is used to estimate the heat flux at the streambed/water interface as given by Hondzo and Stefan (1994). In this method, the heat flux is estimated as the rate of change in the streambed heat storage, which is obtained by integration of the streambed temperature profile. For the 1D case, it can be formulated as

$$H_{sed} = \rho_s c_p \frac{\partial}{\partial t} \int_0^z T_b(z, t) \, dz \qquad (15)$$

Numerical Solution

Eq. (10) is solved by using the MacCormack scheme (Chaudhry 1993). This is an explicit, two-step, predictor-corrector scheme that is second-order accurate in space and time. A description of the method for an unsteady, 1D, free-surface flow is given as follows:

Predictor step:

$$\frac{\partial T}{\partial t} = \frac{T_i^* - T_i^n}{\Delta t}; \quad \frac{\partial T}{\partial x} = \frac{T_i^n - T_{i-1}^n}{\Delta x} \qquad (16a,b)$$

By substitution of (16) into (10), the resulting equation becomes

$$T_i^* = T_i^n - V_i^n \frac{\Delta t}{\Delta x}(T_i^n - T_{i-1}^n) + \frac{\Delta t}{\Delta x^2 A_i^n}[A_i^n D_i^n(T_i^n - T_{i-1}^n)$$

$$- A_{i-1}^n D_{i-1}^n(T_{i-1}^n - T_{i-2}^n)] + \frac{\Delta t q_x^n}{A_i^n}(T_\ell - T_i^n) + \frac{\Delta t H_t^n w_i^n}{C_w \rho_w A_i^n}$$

$$+ \frac{\Delta t H_{sed}^n p_i^n}{C_w \rho_w A_i^n} \qquad (17)$$

where T_i^* = intermediate value for temperature.

Corrector step:

$$\frac{\partial T}{\partial t} = \frac{T_i^{**} - T_i^n}{\Delta t}; \quad \frac{\partial T}{\partial x} = \frac{T_{i+1}^* - T_i^*}{\Delta x} \qquad (18a,b)$$

The substitution of (18) into (10) and simplification of the resulting equation yields

$$T_i^{**} = T_i^n - V_i^n \frac{\Delta t}{\Delta x}(T_{i+1}^* - T_i^*) + \frac{\Delta t}{\Delta x^2 A_i^n}[A_{i+1}^n D_{i+1}^n(T_{i+1}^* - T_i^*)$$

$$- A_i^n D_i^n(T_i^* - T_{i-1}^*)] + \frac{\Delta t q_x^n}{A_i^n}(T_\ell - T_i^*) + \frac{\Delta t H_t^n w_i^n}{C_w \rho_w A_i^n} + \frac{\Delta t H_{sed}^n p_i^n}{C_w \rho_w A_i^n} \qquad (19)$$

where T_i^{**} = intermediate value for temperature after the corrector step. The new value of temperature at unknown time level $n + 1$ is given by

$$T_i^{n+1} = \frac{1}{2}(T_i^* + T_i^{**}) \qquad (20)$$

The Courant-Friedrichs-Lewy condition has to be satisfied for the preceding scheme to be stable (Anderson et al. 1984)

$$C_n = \frac{|V| \pm \sqrt{gd}}{\Delta x/\Delta t} \leq 1 \qquad (21)$$

where C_n = Courant number; d = hydraulic depth (m); Δx = length of discretized channel reach (m); and Δt = time step (s). Moreover, the truncation errors in this scheme produce unnecessary oscillations in the computed results. These oscillations are smoothed by introducing artificial viscosity (Jameson et al. 1981).

Model Input Requirements

The hydrodynamic and heat transport models require meteorological and stream data input. The meteorological data file consists of the weather data that are used in the model to drive water temperature dynamics. The data include hourly average air temperature, relative humidity, wind velocity, atmospheric pressure, cloud cover, and solar radiation. These are commonly available in the Climatological Data reports from the National Weather Service. The stream data input requires (1) morphometry (cross-sectional area, slope); (2) riparian vegetation (average height, distance from the banks and width of canopy); (3) streambed characteristics (thermal conductivity, heat capacity, and roughness coefficient); (4) upstream streamflow and water temperature time series; (5) lateral inflow/outflow; (6) subsurface inflow/outflow; and (7) initial conditions for streamflow, sediment, and water temperatures.

Selected Stream

The hydrodynamics and heat transport models were applied to a reach of about 2.2 km on the Little Pine Creek watershed in Indiana (Fig. 2). The stream has the following characteristics of bottom width 6.0 m, side slope 1.2H:1V, and bottom slope 1.75×10^{-3}. The watershed that feeds this stream covers a 11,681 ha area that is predominantly used for agriculture. The upstream and downstream gauging sections of the reach are called 800W and 825W, respectively. The relatively short stream reach had been selected to exclude major natural tributaries between the gauging stations.

Data Collection

The gauging stations were installed in the stream at the upstream and downstream sites. Each station contained a portable
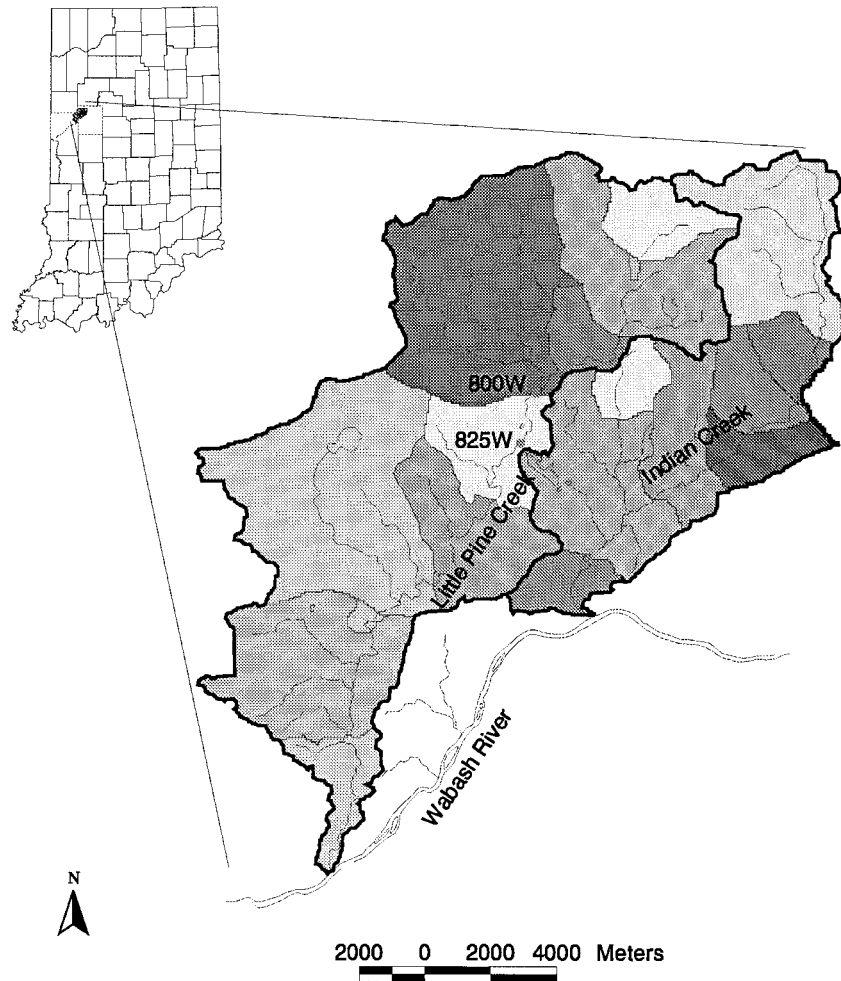
FIG. 2. Little Pine Creek and Indian Creek Watersheds, Ind., 800W (Upstream) and 825W (Downstream) Indicate Location of Gauging Stations on Little Pine Creek

sampler (ISCO), bubbler module for continuous stream stage record (ISCO), data logger (Campbell: CR10), temperature probes, marine battery, and housing. The temperature probes are rubber-coated thermistors with a time constant of 10 s. They were calibrated in a water bath prior to installation. Absolute accuracy (value measured by two adjacent probes at known temperature) was ±0.05°C, and relative accuracy (the difference between successive measurements by the same probe) was 0.01°C. The water and sediment temperatures were recorded every 15 min from May 15 to June 9, 1998. A stage-discharge dependence was established by conducting several velocity-streamflow measurements across the upstream and downstream gauging sites. The ground-water temperatures were measured in a well that is located about 100 m from the downstream gauging station. The water temperatures were recorded every 15 min from May 15 to June 9, 1998. The soil temperature data at 80 cm below the ground surface were obtained from the nearby Agronomy Experimental Station, Purdue University (West Lafayette, Ind.).

Hourly meteorological data were obtained from a local meteorological station. The maximum distance between the meteorological station and the stream is about 3 km. The flat and open plane topography justifies the regional transfer of meteorological data. The stability condition in the hydrodynamics part of the numerical model imposed the required time steps for simulations. The hourly meteorological data as well as the upstream boundary conditions for the water temperature and streamflow were interpolated between the measurements to provide the required data at any time step.
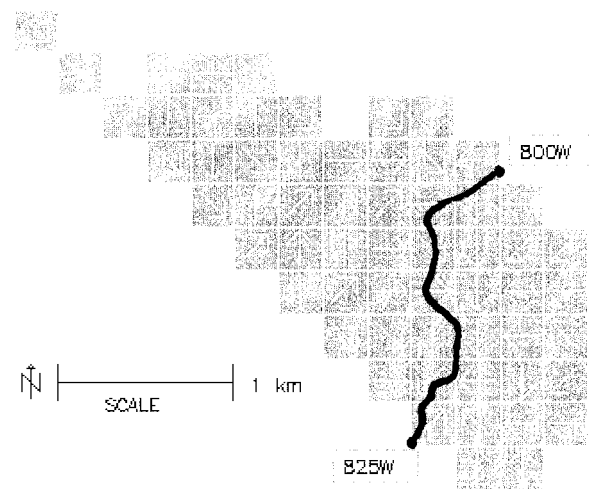

FIG. 3. Flow Direction in Little Pine Creek Subwatershed between Upstream and Downstream Gauging Stations on Little Pine Creek (Bold Line)

RESULTS

Streamflow

The watershed was delineated using the downstream gauging site of the reach as an outlet prior to the numerical simulations. The geographical resources analysis support system/geographic information system was used to analyze the flow
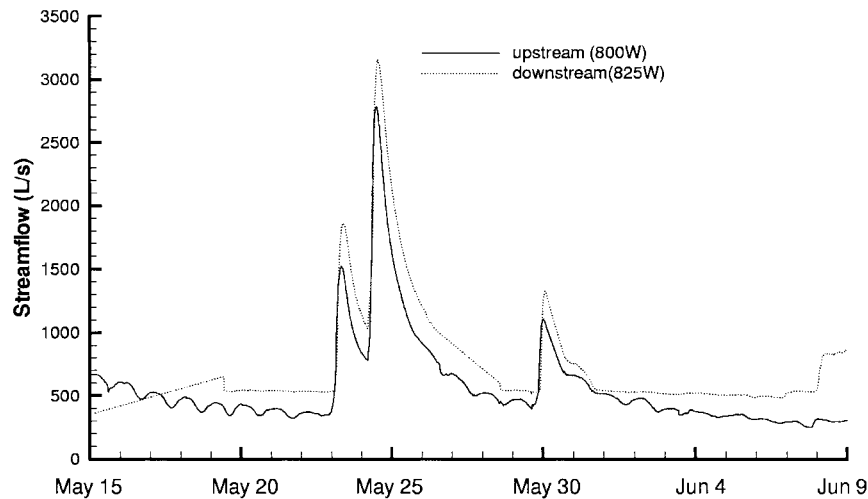
FIG. 4. Measured Short-Term Streamflow (L/s) from May 15 to June 9, 1998, at Stream Gauges on Little Pine Creek
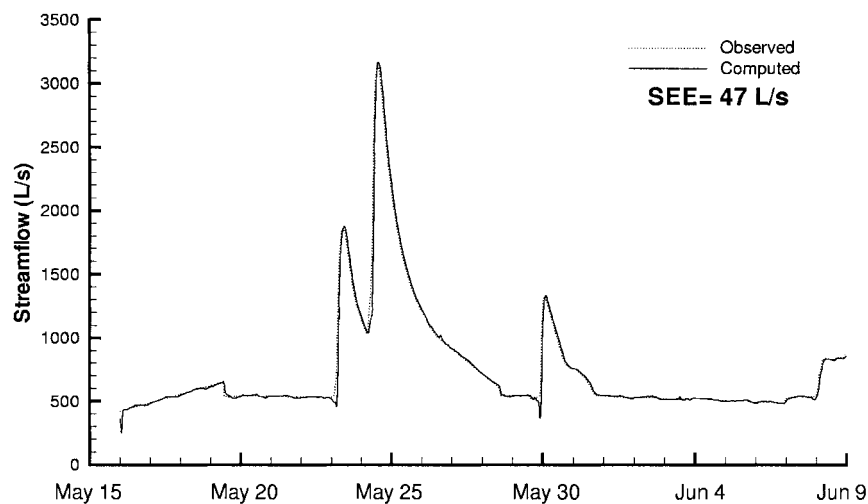

FIG. 5. Comparison of Measured Streamflow (L/s) with Simulated Streamflow (L/s) from May 15 to June 9, 1998, at Downstream Gauging Station on Little Pine Creek

path from the land surface in the subwatershed between the upstream and downstream measuring sites (Fig. 3). The raster cells (250 × 250 m) indicate the surface areas in the watershed that may contribute to the stream reach between the upstream and downstream stations. The arrows indicate the flow direction in each raster cell. It can be seen that a negligible amount of surface runoff is contributed to the stream reach between the upstream (800W) and the downstream (825W) stations.
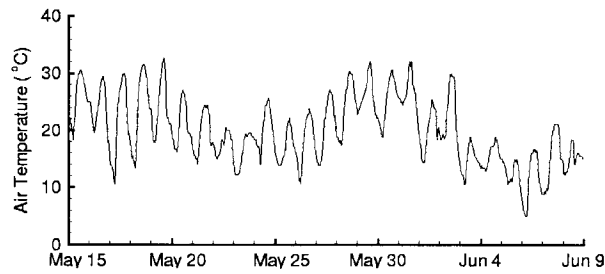
The observed hydrographs for the upstream and the downstream stations are given in Fig. 4. Diurnal variations in flow rates were significant. The downstream station (825W) displays higher flow rates than the upstream measuring site. The difference between the streamflows, lagged by the travel time, is mainly caused by the subsurface flows. Ground-water flow, tile drain flow, and the infiltrated rainfall through the soil are examples of possible pathways that may contribute to the subsurface flow in the agricultural watersheds. Traditionally, agricultural watersheds are equipped with subsurface tile drains. The tile drains, located about 80 cm below the ground surface, lower the moisture content of the upper soil and accelerate soil damage. The tile flows contribute significantly to a streamflow in the upland agricultural watersheds (Kim 1996). Several tile drains are observed between the upstream and downstream stations in the watershed along Little Pine Creek.

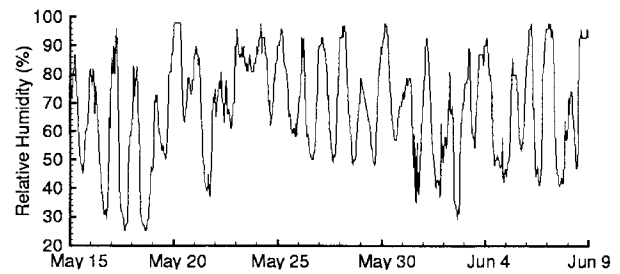The model was verified using the measured streamflow at

the upstream and downstream sites from May 15 to June 9, 1998. A Δx of 30 m was used in this simulation with an averaged constant cross-sectional area at all the nodes. The subsurface flow was computed by subtracting the measured upstream flow from the downstream flow. The subsurface flow was assumed to be evenly distributed over the length of the reach. An average subsurface flow of 0.086 L/s/m is estimated from the difference between the observed streamflows. The upstream hydrograph was used as a boundary condition in the hydrodynamics part of the model. The initial condition was computed by the interpolation of the measured flow rate at upstream and downstream stations. Fig. 5 shows the comparison between the observed and computed streamflows at the downstream site (825W). The streamflows were almost identical. The flow rate ranged from 400 to 3,200 L/s during the simulation period. There was good agreement between the simulated and observed streamflows.
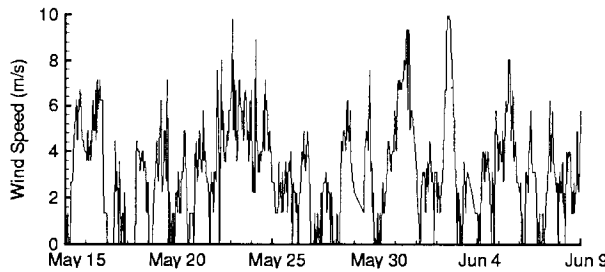
Water Temperature

The hourly meteorological data time series that are measured from May 15 to June 9, 1998, are given in Fig. 6. The data display daily cycles over 25 days. The diurnal stream temperature variation followed the diurnal cycles of solar radiation and air temperature (Fig. 7). The water temperature
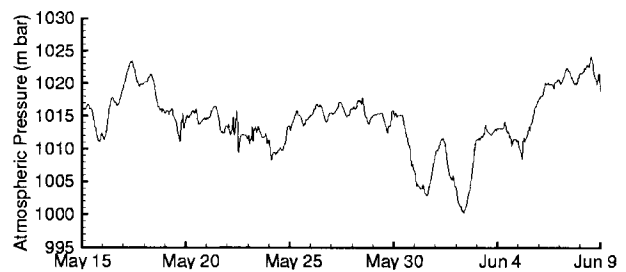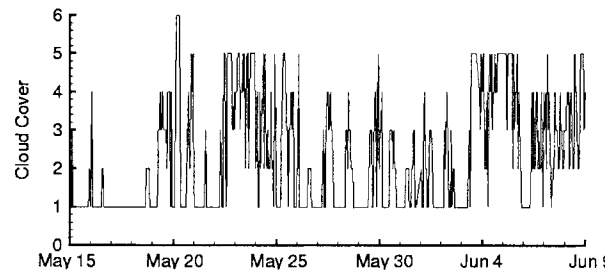
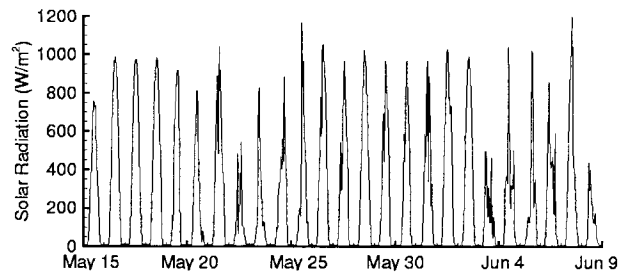(a) Air temperature

(b) Relative humidity

(c) Wind velocity

(d) Atmospheric pressure

(e) Cloud cover

(f) Solar radiation

FIG. 6. Observed Hourly Meteorological Data from May 15 to June 9, 1998, for Little Pine Creek Watershed

ranged from 14 to 22°C. The effect of heat exchange between the stream and its surroundings can be seen by comparing water temperatures measured at upstream and downstream stations. The maximum difference between the upstream and downstream temperatures was 2.9°C. The difference between the two-lagged time series indicate that there is a heat loss from the stream (Fig. 7). The sediment temperature measurements in the stream are given in Fig. 8. The probes located 30 cm below the sediment-water interface depicted the subdaily and daily stream water temperature variability. The groundwater temperature was a constant 10°C over the measurement period. It has been recognized by a number of researchers that a strong temperature signature is present in the sediment of a stream, if the stream strongly gains ground water (Nelson 1991; Silliman and Booth 1993). The measured water and sediment temperature (Figs. 7 and 8) indicated that the stream falls in the category of very little interchange of the water between stream and ground water (Silliman and Booth 1993). Consequently, the difference in streamflow between the upstream and downstream stations is contributed by subsurface flow from tile drains.

The effective thermal conductivity k and the streambed heat capacity $\rho_s c_p$ were the calibration coefficients in the heat trans-

port model. The parameters were estimated from the streambed temperature measurements (Fig. 8) as indicated in studies by Sinokrot and Stefan (1993) and Hondzo and Stefan (1994). The optimum values of $k = 1.44$ Wm^{-1} °C^{-1} and $\rho_s c_p = 2.75 \times 10^6$ J m^{-3} °C^{-1} simulated the observed streambed temperatures with comparable accuracy as reported in the above studies.

The thermal transport part of the model was verified using the measured water temperatures at the upstream and downstream sites from May 15 to June 9, 1998. The observed upstream water temperatures were used as a boundary condition. The measured soil temperature at the tile drain elevation, 80 cm below the ground surface, was a constant 15°C over the measurement period, and the calculated subsurface flows were used as the lateral subsurface flow along the stream. The initial condition was computed by the interpolation of the measured water temperature at the upstream and downstream stations. Fig. 9 shows the comparison between the observed and simulated water temperatures at the downstream site (825W). The model predicted the diurnal variability of the water temperatures well. The standard error of estimation (SEE) was 0.7°C for the temperature range from 12 to 23°C. The upstream boundary is sometimes not available in practice and, therefore,
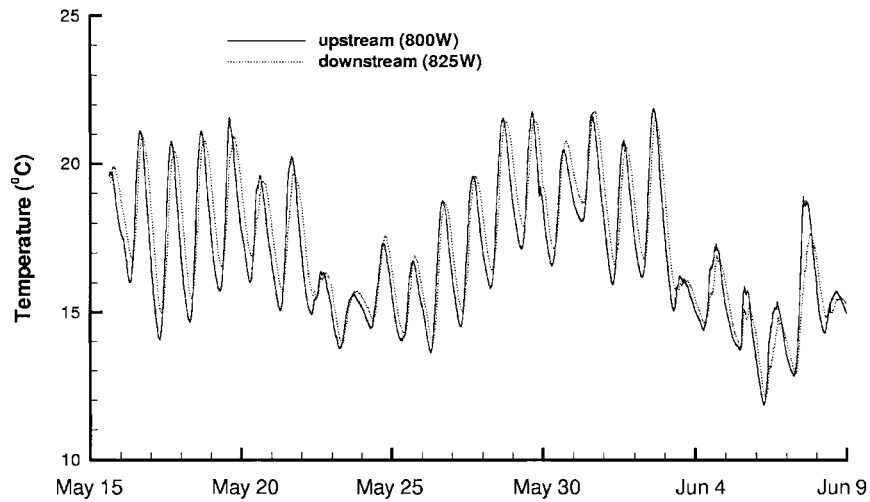
FIG. 7. Measured Short-Term Water Temperature (°C) from May 15 to June 9, 1998, at Stream Gauges on Little Pine Creek
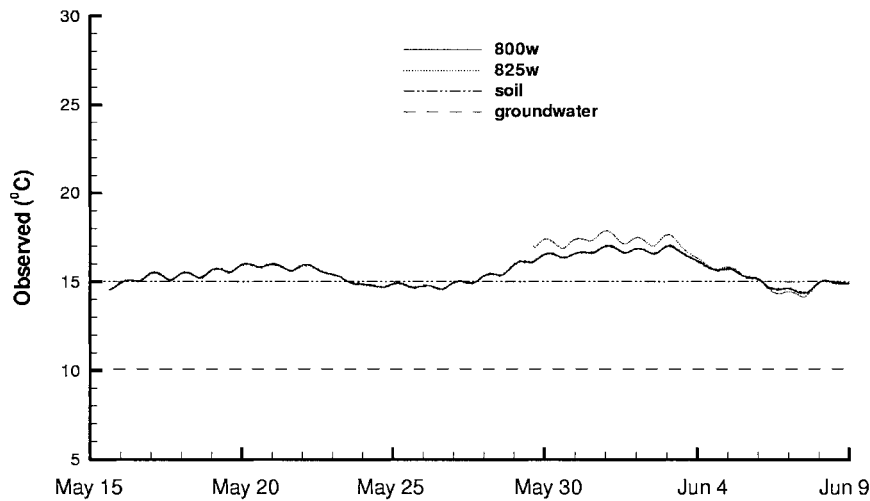

FIG. 8. Measured Short-Term Sediment, Ground Water, and Soil Temperature (°C) at Tile Drain Elevation from May 15 to June 9, 1998, at Stream Gauges on Little Pine Creek
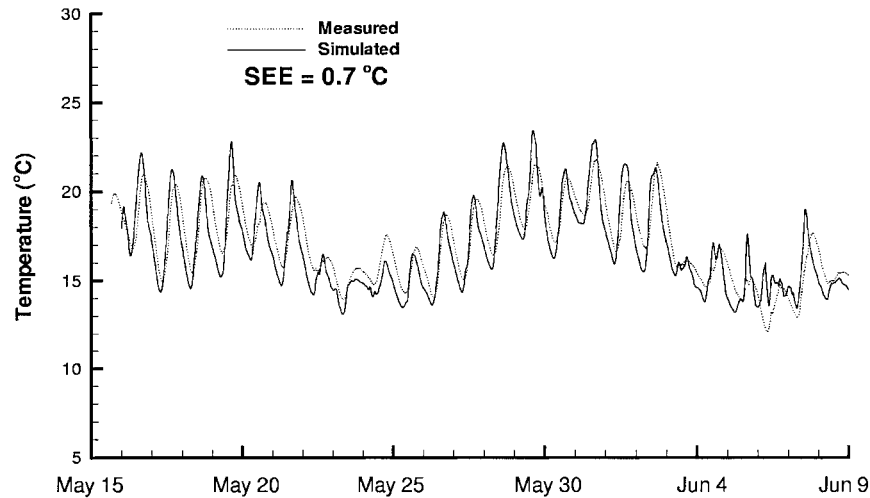

FIG. 9. Comparison of Measured Water Temperature (°C) with Simulated Water Temperature (°C) by Using Measured Upstream Boundary Condition from May 15 to June 19, 1998, at Downstream Gauging Station on Little Pine Creek

has to be estimated. The concept of "a freely flowing stream" was used to estimate the upstream boundary condition (Sinokrot and Stefan 1993). This concept implies that a time change of water temperature within a well-mixed water column is equal to a heat exchange between the water and a surrounding environment. The simplified heat transport equation takes the form

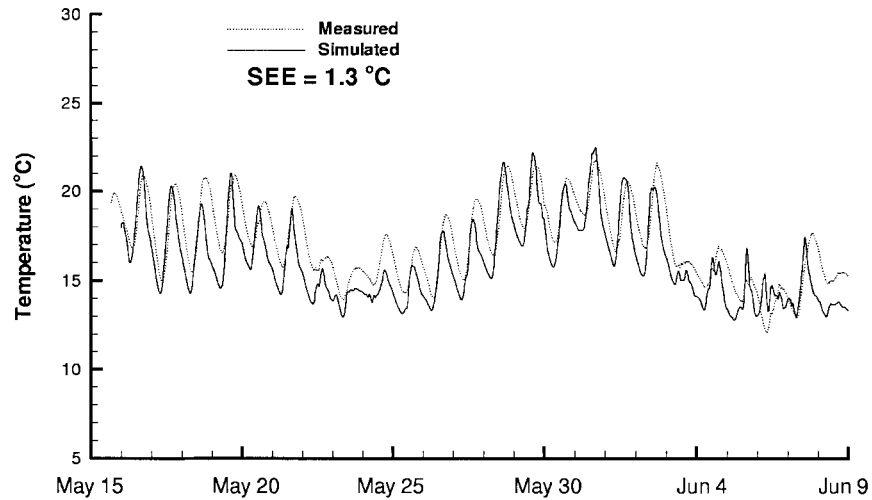$$\frac{\partial T}{\partial t} = \frac{H_t}{C_w \rho_w y} \qquad (22)$$

FIG. 10. Comparison of Measured Water Temperature (°C) with Simulated Water Temperature (°C) by Using Simulated Upstream Boundary Condition from May 15 to June 9, 1998, at Downstream Gauging Station on Little Pine Creek
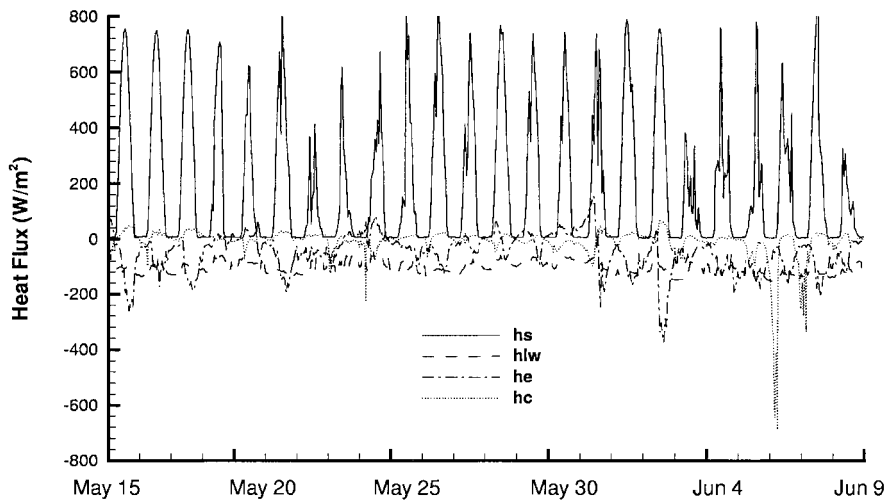

FIG. 11. Comparison among Computed Heat Flux Components (W/m^2) of Solar (Shortwave) Radiation (h_s), Longwave Radiation (h_{lw}), Evaporation (h_e), and Convection (h_c) from May 15 to June 9, 1998, at Downstream Gauging Station on Little Pine Creek
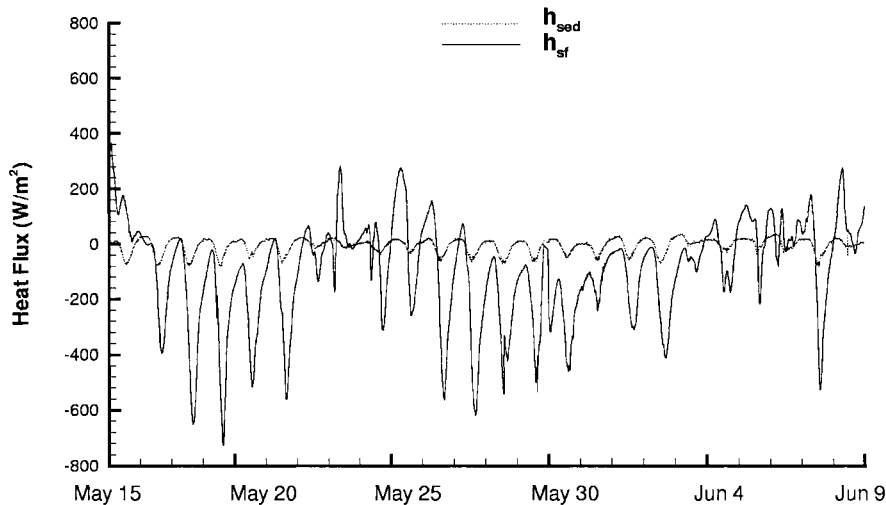

FIG. 12. Comparison between Computed Sediment Heat Flux h_{sed} (W/m^2) and Subsurface Flow Heat Flux h_{sf} (W/m^2) from May 15 to June 9, 1998, at Downstream Gauging Station on Little Pine Creek

where y = mean flow depth (m). Eq. (22) was solved using the fourth-order Runge-Kutta method. Fig. 10 shows the comparison between the observed and predicted water temperatures, with a simulated upstream boundary condition at the downstream site. The SEE was 1.3°C.

Heat Flux Components

The heat budget of a stream is primarily determined by heat exchange between water surface and atmosphere, water and sediment, inflows, and outflows. Secondary heat inputs are

through chemical reactions, plant and animal metabolism, and viscous dissipation. Examples of the primary heat budget components are plotted for Little Pine Creek in Figs. 11 and 12. The positive heat flux corresponds to an energy source whereas the negative heat flux is an energy sink in the water column. The shortwave radiation was the dominant heat budget component in the water surface-atmosphere heat exchange (Fig. 11). The heat flux displayed daily on-off cycles during the simulation period. The streambed heat flux depicted daily variability in response to the streambed-water temperature changes (Fig. 9). The flux was either negative or close to zero and, therefore, acted as a sink term in the heat budget. The magnitude of the flux was comparable to the heat fluxes caused by the longwave radiation and evaporation. The heat flux caused by subsurface flow was on average an energy sink in the heat budget (Fig. 12). The flux is proportional to the subsurface flow and the temperature difference between the streamflow and subsurface flow. In magnitude, the flux was comparable to the shortwave radiation heat flux.

CONCLUSIONS

The flow rates in streams, located in agricultural watersheds, are highly transient. The continuous flow rate records showed diurnal variations in streamflows from 800 to 8,000 L/s. The diurnal variations in stream temperatures were from 14 to 20°C. The ground-water temperature was a constant 10°C over subdaily and daily timescales from May 15 to June 30, 1998.

A numerical model based on full hydrodynamics and heat transport equations was formulated to predict streamflows and water temperatures. A hydrodynamics model accounts for the effects of arbitrary creek geometry, variable slopes, variable flow regimes, and unsteady boundary conditions. A thermal transport model accounts for the effects of solar radiation, air temperature, relative humidity, cloud cover, wind speed, heat conduction between water and streambed, subsurface flow, and shading by riparian vegetation. The proposed hydrodynamic model predicts streamflows at time steps <1 h over 25 days with high accuracy. The thermal transport model predicts water temperatures at the above duration and time steps with the accuracy on the order of 0.7°C.

The results of this study demonstrate that the solar (shortwave) radiation and the subsurface flow caused by tile drains are the most significant contributors in the stream heat budget. The concept of direct coupling among stream temperature, streamflow, and ground-water exchange was reported for alpine streams (Contantz 1998). The measurements and numerical simulations conducted in this study confirm the above concept, such that the increased streamflows by the subsurface flow decreased stream temperatures. Although the stream is shallow, sediment heat flux was not significant, but comparable to heat fluxes caused by longwave radiation and evaporation.

ACKNOWLEDGMENTS

APPENDIX.   REFERENCES

Abbot, M. B. (1979). *Computational hydraulics: Elements of the theory of free surface flow.* Pitman Publishing Ltd., London.

Anderson, D. A., Tannehill, J. C., and Pletcher, R. H. (1984). *Computational fluid mechanics and heat transfer.* McGraw-Hill, New York.

Beam, R. M., and Warming, R. F. (1976). "An implicit finite-difference algorithm for hyperbolic systems in conservation-law form." *J. Comp. Phys.*, 22, 87–110.

Beam, R. M., and Warming, R. F. (1978). "An implicit factored scheme for compressible Navier-Stokes equations." *AIAA J.*, 16(4), 393–402.

Chapra, S. C. (1997). *Water quality modeling.* McGraw-Hill, New York.

Chaudhry, M. H. (1993). *Open channel flow.* Prentice-Hall, Englewood Cliffs, N.J.

Chen, Y. D., Carsel, R. F., McCutcheon, S. C., and Nutter, W. L. (1998a). "Stream temperature simulation of forested riparian areas: 1. Watershed-scale model development." *J. Envir. Engrg.*, ASCE, 124(4), 304–315.

Chen, Y. D., McCutcheon, S. C., Norton, D. J., and Nutter, W. L. (1998b). "Stream temperature simulation of forested riparian areas: II. Model applications." *J. Envir. Engrg.*, ASCE, 124(4), 316–328.

Contantz, J. (1998). "Interaction between stream temperature, stream flow, and ground water exchange in alpine streams." *Water Resour. Res.*, 34(7), 1609–1615.

Fennema, R. J., and Chaudhry, M. H. (1987). "Simulation of one-dimensional dam-break flows." *J. Hydr. Res.*, Delft, The Netherlands, 25(1), 41–51.

Fennema, R. J., and Chaudhry, M. H. (1989). "Implicit methods for two-dimensional unsteady free-surface flows." *J. Hydr. Res.*, Delft, The Netherlands, 27(3), 321–332.

Holley, E. R., and Jirka, G. H. (1986). "Mixing in rivers." *Tech. Rep. AD/A174 931*, Nat. Tech. Information Service., U.S. Department of Commerce.

Hondzo, M., and Stefan, H. G. (1994). "Riverbed heat conduction prediction." *Water Resour. Res.*, 30(5), 1503–1513.

Jameson, A., Schmidt, W., and Turkel, E. (1981). "Numerical solution of the Euler equations by finite volume methods using Runge-Kutta time-stepping schemes." *Proc., AIAA 14th Fluid and Plasma Dyn. Conf.*, AIAA, Washington, D.C.

Kim, K. S., and Chapra, S. C. (1997). "Temperature model for highly transient shallow streams." *J. Hydr. Engrg.*, ASCE, 123(1), 30–40.

Kim, S. (1996). "Hydrologic and water quality modeling of agricultural watersheds equipped with tile drains using a geographic information system and fractal concepts." PhD thesis, Purdue University, West Lafayette, Ind.

Mohseni, O., Stefan, H. G., and Erickson, T. R. (1998). "A nonlinear regression model for weekly stream temperature." *Water Resour. Bull.*, 34(10), 2685–2692.

Nelson, J. (1991). "Analysis of thermal scanning imagery and physical sampling to investigate point inflows to surface bodies." MS thesis, University of Notre Dame, Notre Dame, Ind.

Polehn, R. A., and Kinsel, W. C. (1997). "Transient temperature solution for stream flow from a controlled temperature source." *Water Resour. Res.*, 33(1), 261–265.

Rasmussen, A. H., Hodzo, M., and Stefan, H. G. (1995). "A test of several evaporation equations for water temperature simulations in lakes." *Water Resour. Bull.*, 31(6), 1–6.

Ronan, A. D., Prudic, D. E., Thodal, C. E., and Constantz, J. (1998). "Field study and simulation of diurnal temperature effects on infiltration and variably saturated flow beneath an ephemeral stream." *Water Resour. Res.*, 34(9), 2137–2153.

Silliman, S. E., and Booth, D. F. (1993). "Analysis of time-series measurements of sediment temperature for identification of gaining vs losing portions of Juday Creek, Indiana." *J. Hydro.*, Amsterdam, 146, 131–148.

Sinokrot, B. A., and Stefan, H. G. (1993). "Stream temperature dynamics: Measurements and modeling." *Water Resour. Res.*, 29(7), 2299–2312.

Stefan, H. G., and Preud'homme, E. (1993). "Stream temperature estimation from air temperature." *Water Resour. Bull.*, 29(1), 27–45.

Theurer, F. D., Voos, K. A., and Miller, W. J. (1984). "Instream water temperature model." *FWS/OBS-84/15*, U.S. Fish and Wildlife Service, Washington, D.C.

Warming, R. F., and Beam, R. M. (1978). "On the construction and application of implicit factored schemes for conservation laws." *Proc., Symp. on Computational Fluid Dyn.*, Vol. 11, Society for Industrial and Applied Mathematics-AMS, 85–129.

Webb, B. W., and Nobilis, F. (1997). "Long-term perspective on the nature of the air-water temperature relationship: A case study." *Hydrological Processes*, England, 11(1), 137–147.

Younus, M., and Chaudhry, M. H. (1994). "A depth-averaged turbulent model for the computation of free-surface flow." *J. Hydr. Res.*, Delft, The Netherlands, 32(3), 415–444.